EPJ manuscript No.
(will be inserted by the editor)

Effect of a sweeping conductive wire on electrons stored in a Penning-like trap between the KATRIN spectrometers

M. Beck[1], K. Valerius[1a], J. Bonn[2], K. Essig[3], F. Glück[4,5], H.-W. Ortjohann[1], B. Ostrick[1,2], E. W. Otten[2], Th. Thümmler[3b], M. Zbořil[1,6], and C. Weinheimer[1,3]

[1] Institut für Kernphysik, Westfälische Wilhelms-Universität Münster, Germany
[2] Institut für Physik, Johannes Gutenberg-Universität Mainz, Germany
[3] Helmholtz-Institut für Strahlen- und Kernphysik, Rheinische Friedrich-Wilhelms-Universität Bonn, Germany
[4] Institut für Experimentelle Kernphysik, Karlsruhe Institute of Technology, Germany
[5] Res. Inst. Nucl. Part. Phys., Budapest, Hungary
[6] Nuclear Physics Institute ASCR, Řež near Prague, Czech Republic

the date of receipt and acceptance should be inserted later

Abstract. The KATRIN experiment is going to search for the mass of the electron antineutrino down to $0.2\,\mathrm{eV/c^2}$. In order to reach this sensitivity the background rate has to be understood and minimised to 0.01 counts per second. One of the background sources is the unavoidable Penning-like trap for electrons due to the combination of the electric and magnetic fields between the pre- and the main spectrometer at KATRIN. In this article we will show that by sweeping a conducting wire periodically through such a particle trap stored particles can be removed, an ongoing discharge in the trap can be stopped, and the count rate measured with a detector looking at the trap is reduced.

PACS. 14.60.Pq Neutrino mass and mixing – 23.40.-s Beta decay; double beta decay; electron and muon capture – 29.30 Electron spectroscopy – 52.80 Magnetoactive discharges

arXiv:0909.3337v2 [physics.ins-det] 3 Oct 2010

1 Motivation

In light of the confirmation of neutrino oscillations by many experiments in the last decade, the question of the absolute mass scale of neutrinos is very important for particle physics and cosmology (see *e.g.*, [1,2]). The KArlsruhe TRItium Neutrino experiment (KATRIN, [3]) aims to search for the mass of the electron antineutrino with a sensitivity of $0.2\,\mathrm{eV/c^2}$. At KATRIN electrostatic energy filters of MAC-E filter type (electrostatic filter with magnetic adiabatic collimation, [4,5]) are used both for the precision measurement of the endpoint of the beta decay of tritium with the main spectrometer, and for the reduction of the bulk of the electrons at energies of approx. 200 eV below the endpoint with the pre-spectrometer, which is located upstream of the main spectrometer (see fig. 1).

A spectrometer of MAC-E filter type consists of an electrostatic retardation potential, acting as a high pass filter, combined with an inhomogeneous magnetic guiding field. Two superconducting solenoids produce a strong magnetic field B_{max} at the entrance and exit of the spectrometer. The magnetic field strength decreases towards the centre of the spectrometer to a minimum value[1] B_{min}. This results in an expansion of the magnetic flux tube towards the centre of the spectrometer. Due to the magnetic gradient force the radial energy $E_\perp$ of an electron that moves adiabatically into this weak field area is converted nearly completely into longitudinal energy $E_\parallel$ according to the conservation of the magnetic orbital momentum

$$\mu = \frac{E_\perp}{B} \tag{1}$$

(equation given in the non-relativistic limit). The longitudinal energy is then probed by the electric potential U_{spec} in the analysis plane at $B = B_{\mathrm{min}}$ and $z = 0$ (see fig. 1). Only electrons with sufficient longitudinal kinetic energy, $E_\parallel > qU_{\mathrm{spec}}$, with $q = -e$ being the electron charge, will be able to pass the filter and get re-accelerated towards the detector at the exit of the spectrometer.

To reach the proposed sensitivity at KATRIN the background rate at the endpoint of the tritium beta decay has to be minimised. One background component at KATRIN stems from particle traps that exist due to the combination of the high electric and magnetic fields of the MAC-E filters themselves. Through ionisation processes a trapped

[a] Present address: Physikalisches Institut, Friedrich-Alexander-Universität Erlangen-Nürnberg, Germany
[b] Present address: Institut für Kernphysik, Karlsruhe Institute of Technology, Germany
Correspondence to: marcusb@uni-muenster.de

[1] In the KATRIN set-up, this reduction factor $B_{\mathrm{max}}/B_{\mathrm{min}}$ amounts to 20000.

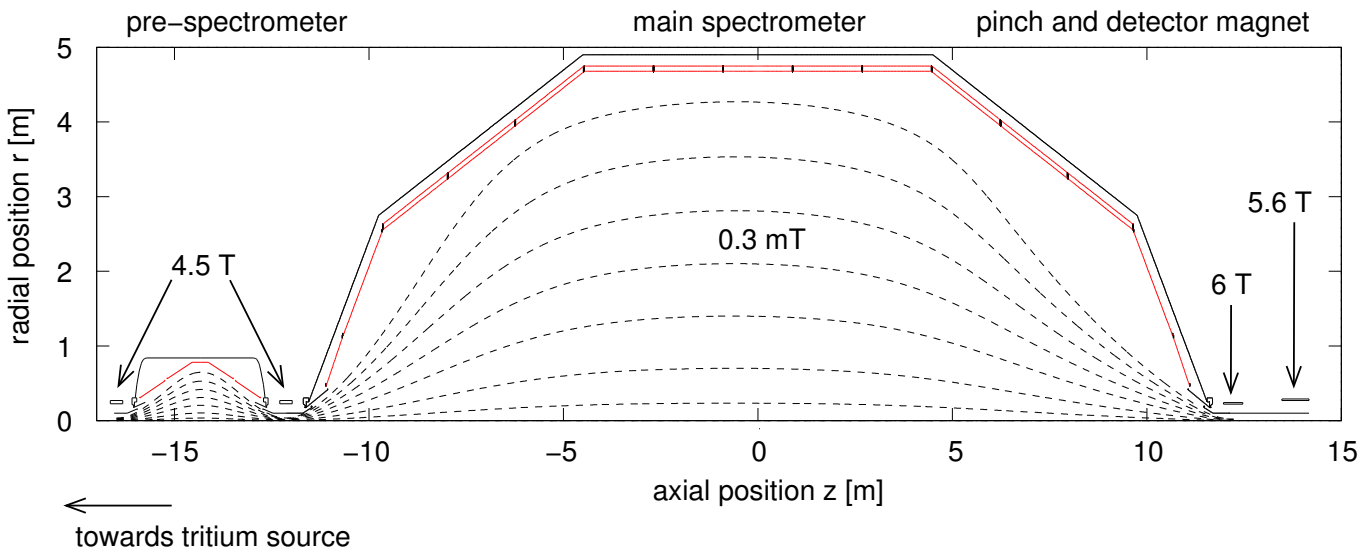


Fig. 1. Overview of the two-spectrometer set-up of the KATRIN experiment (left: small pre-spectrometer, right: large main spectrometer) and its magnetic fields according to the present KATRIN default configuration. Note that in the original KATRIN design [3] two short solenoids and a 3 m long magnetic transport section were foreseen between the two spectrometers. These two transport magnets are replaced by a single short solenoid in the present KATRIN default configuration. Dashed lines represent magnetic field lines. The field lines in the main spectrometer are shaped by an air coil system which is not shown. High voltage of the order of -18.6 kV is applied in the centre (weak magnetic field) regions of the spectrometers (pre-spectrometer: $z \approx -15$ m, main spectrometer: $z \approx 0$ m). At the magnet between the spectrometers at $z = -12$ m the electric potential is zero. In combination with the magnetic field this potential well creates a large Penning-like trap for electrons between the pre- and the main spectrometer.

particle can cause an increase of the number of charged particles, which in turn may give rise to an enhanced background count rate.

One type of particle trap of particular importance for KATRIN is the Penning trap [6]. In a Penning trap charged particles are confined by a magnetic field in radial direction. The confinement in axial direction is achieved by an electrostatic potential (see fig. 2). The MAC-E filter for electrons with its negative central potential and both sides at ground potential together with the axial magnetic field constitutes a large Penning-like trap for positively charged particles. Light positively charged particles do not exist in the KATRIN experiment[2] and for more massive positively charged particles, *e.g.*, protons, the cyclotron radii typically get too large so that the charged particles can escape radially.

Penning-like traps for electrons, however, can easily be created at various locations inside the MAC-E filter. Great care has to be taken in the design of the electric and magnetic fields in order to avoid these traps [7,8]. In a two-spectrometer set-up like the one formed by the KATRIN pre- and main spectrometer, such a trap for electrons cannot be avoided in principle. The two negative retarding potentials together with the high magnetic field between them form a large Penning-like trap for electrons (compare fig. 1).

In this paper we will focus on the particular kind of electron trap caused by the combination of the two spectrometers of MAC-E filter type. We will report in section 2 on our first estimates whether and how this trap could cause a significant background rate at the KATRIN experiment. In sections 3 and 4 we will present our experimental set-up and the investigations of our new method to periodically empty this electron trap in order to reduce the background rate which may originate from electrons stored in this trap. In section 5 we will give our conclusions.

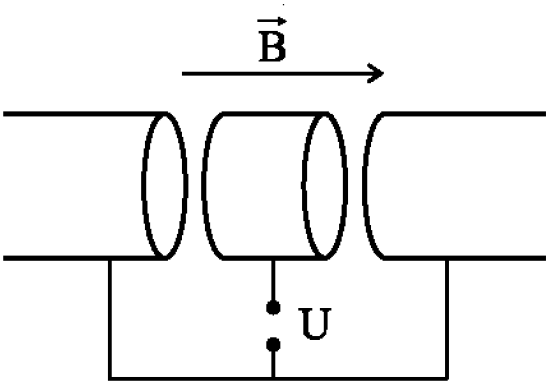


Fig. 2. Principle of a cylindrical Penning trap. The electrons are confined by an electrostatic potential U in axial direction and by a B-field in radial direction.

[2] There is no known source of positrons at KATRIN.

2 Background from the inter-spectrometer trap

We expect that the electron trap, which is formed by the combination of the pre- and the main spectrometer of KATRIN, will be filled from the outside at a rate comparable to the total background rate on the detector, which is expected to be ≈ 0.2 counts/s[3]. These electrons confined within the inter-spectrometer trap are not a direct source of background, but can produce indirect background at the KATRIN detector. Three known processes could create such background. Two of them are connected to ionisation processes in the trap and positively charged ions leaving the trap towards the main spectrometer, where they produce secondary electrons in the volume or at the walls. The third process starts with a photon from deexcitation or recombination processes in the trap, which creates also secondary electrons in the main spectrometer. All three processes may yield similar background rates and studies of these effects are still in progress. In the following we will elaborate on the first process, background electrons from ionisation of rest gas due to ions from the trap. This is a two-step process:

1. An electron stored in the trap interacts with the residual gas, creating a secondary electron and a positively charged ion. In most cases the former will get trapped, as well. The latter, which usually will be a proton (H^+) or a H_2^+, will leave the trap and will be accelerated by the electric field towards either the pre- or the main spectrometer.
2. In the low magnetic field $B_{\min} = 0.3$ mT in the centre of the main spectrometer the cyclotron radius of the ion will become too big and hence the ion will not be guided adiabatically by the magnetic field. Thus it will be lost by hitting a spectrometer wall[4], as confirmed by our particle tracking simulations[5]. On its about 20 m long way until hitting the wall it has only a minor chance to cause a second ionisation. But if this happens in the high retarding potential of the main spectrometer, there is a 50 % chance that the created tertiary electron will follow the gradient of the electric field towards the detector exit of the main spectrometer and be counted as a background electron. Due to the limited energy resolution of the electron detector ($\Delta E_{\mathrm{det}} \approx 1$ keV) this electron cannot be distinguished from a signal electron, because it will reach the detector with a kinetic energy given by the sum of its energy at creation $E_{\mathrm{start}} = \mathcal{O}(10)$ eV and the retarding potential $qU = 18.6$ keV. Since the signal electrons from the endpoint region of tritium beta decay with an energy a little bit above the retarding potential qU have about the same energy they cannot be distinguished from these background electrons.

The cross section for the processes

$$H^+ + H_2 \rightarrow e^- + X, \qquad H_2^+ + H_2 \rightarrow e^- + X \tag{2}$$

amounts to $\sigma_{\mathrm{ion}} \approx 10^{-16}$ cm^2 at $E_{\mathrm{ion}} \approx 18.6$ keV [9]. This cross section results in an ionisation probability P_{ion} for an ion track length of $l = 20$ m and a residual gas pressure[6] of $p = 10^{-11}$ mbar ($n(H_2) = 2.5 \cdot 10^{11}/\mathrm{m}^3$) of

$$P_{\mathrm{ion}} = \sigma_{\mathrm{ion}} \cdot n \cdot l = \frac{\sigma_{\mathrm{ion}} \cdot p \cdot l}{k_{\mathrm{B}} \cdot T} = 5 \cdot 10^{-8} \tag{3}$$

This probability is very low and one might tend to neglect the described chain of processes in case there is no other multiplication process. However, a secondary electron created by the first ionisation in the trap has a significant chance of being created in a high potential at either end of the trap, the reason being that the ionisation cross section is highest when the primary electron is low in energy. This condition is fulfilled close to the reflecting retardation potential. In this case the secondary electron gains enough energy in the electric potential to perform another ionisation itself. Therefore, we have to check how many ionisations N_{ion} in the trap can be traced back to a single trapped electron. If N_{ion} is of order $1/P_{\mathrm{ion}}$ this chain of background processes could lead to a significant background rate at the detector.

In the following, we report on first trajectory simulations of electrons in this Penning-like inter-spectrometer trap including cooling processes by synchrotron radiation as well as by elastic and inelastic scattering of electrons off the residual gas [10].

The electron tracking calculations (an example is shown in fig. 3) were performed with the program package Adipark [11] using the guiding-centre approximation: In zeroth approximation the β electrons are spiralling around the guiding magnetic field lines. Therefore, we used the magnetic field lines calculated by the program Bfield3d [12] to propagate the electrons, while adjusting the energy according to the local electrostatic field as computed

[3] At the Mainz neutrino mass experiment the background rate in the energy window of interest was of order 0.01 counts/s, whereas the background over the full energy range amounted to about 0.1 counts/s. Although the KATRIN pre- and main spectrometer are larger and hence should exhibit a larger background, we expect that the advanced electrostatic shielding by a wire electrode system [3,7] will allow to keep the spectrometer-related background rate at the same level as in the Mainz experiment. For the considerations presented in this paper we thus assume that the two KATRIN spectrometers will emit electrons towards both of their ends at a rate comparable to the 0.1 counts/s determined at Mainz.

[4] When hitting the wall the ion could eject a secondary electron, which has a very small chance to reach the detector. This is the second background processs mentioned above. The natural magnetic shielding of a MAC-E filter together with the electric shielding by a two-layer wire electrode system [3,7] suppress this process by about 7 orders of magnitude.

[5] Ions from the trap that reach the pre-spectrometer will not be trapped there either, since they will have gained sufficient energy in the electric potential to move non-adiabatically and will therefore hit the pre-spectrometer electrodes or wall and thus will be removed from the trap.

[6] At the ultra-high vacuum level of the KATRIN experiment the residual gas mainly consists of H_2 molecules.

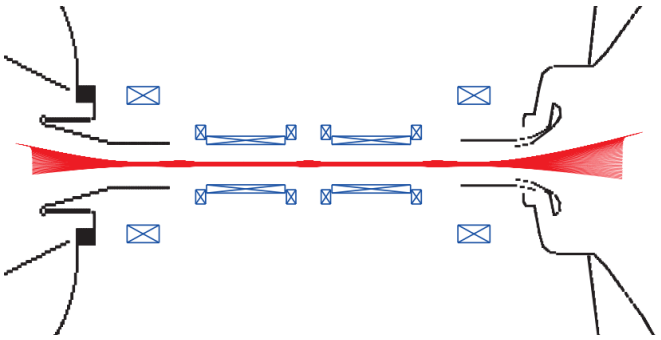


Fig. 3. Example of a tracking simulation of a trapped electron in the inter-spectrometer electron trap [10]. The experimental set-up corresponds to the description in the KATRIN design report [3] with two 2 m long transport magnets (B = 5.4 T) and two short solenoids.

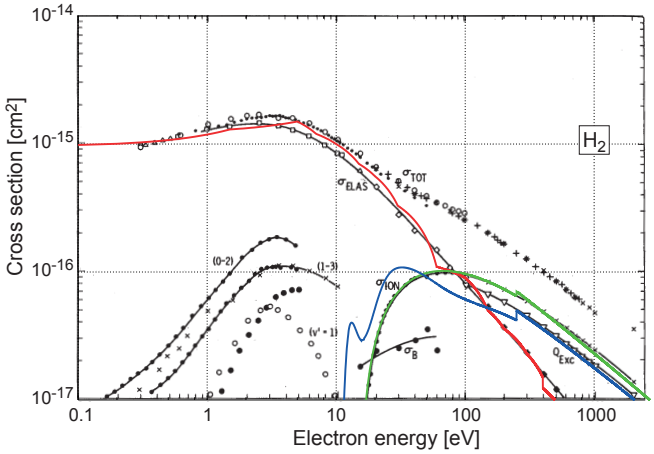


Fig. 4. Comparison of the total cross sections used in our simulation with experimental data [15]. The total cross sections for elastic processes of electrons on H_2 molecules are shown in red, for molecular excitation in blue and for ionisation in green [10].

by the program SimIon 7.0 [13]. Additionally, in non-homogeneous electric and magnetic fields the electrons feel a small drift u, which to first order [4] ($c = 1$) reads

$$\boldsymbol{u} = \left(\frac{\boldsymbol{E} \times \boldsymbol{B}}{B^2} - \frac{(E_\perp + 2E_{||})}{e \cdot B^3} (\boldsymbol{B} \times \nabla_\perp \boldsymbol{B}) \right). \quad (4)$$

It results in a motion transverse to the above-mentioned component along the magnetic field line. In each tracking step the energy loss by synchrotron radiation was taken into account by using the continuous synchrotron radiation formula [14]

$$\frac{1}{\tau_{\mathrm{Sy}}} = \frac{\dot{E}_\perp}{E_\perp} = 0.4\ \mathrm{s}^{-1} \cdot \left(\frac{B}{1\ \mathrm{T}} \right)^2. \quad (5)$$

The elastic and inelastic scattering on the H_2 molecules of the residual gas is simulated as a random process using the total cross sections from refs. [15,16] for elastic scattering, [17,18] for molecular excitation, and [19,20] for

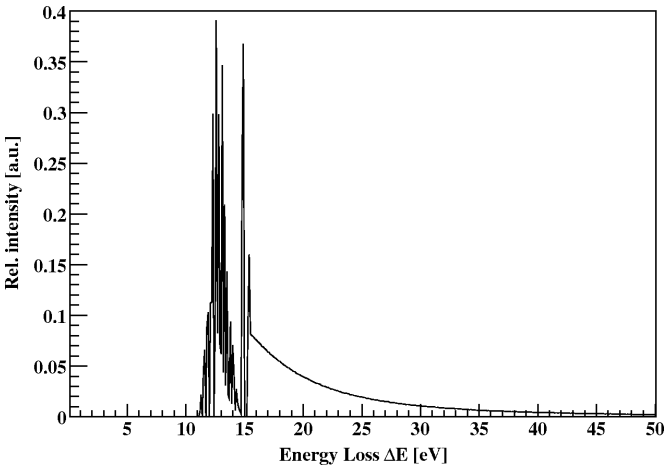


Fig. 5. Energy loss ΔE for molecular excitations and ionisations of 18 keV electrons on H_2 averaged over all scattering angles ϑ according to our energy loss model [21,22].

ionisations. Figure 4 compares these cross sections with experimental data. Each scattering process is related to an energy loss ΔE and a scattering angle ϑ, which can be described by a detailed energy loss model (see fig. 5) to be discussed in a forthcoming publication [22]. As the transverse energy rapidly decreases due to synchrotron radiation, special care has been taken with regard to the realistic description of the scattering angle. For elastic scattering the correlation between energy loss ΔE and scattering angle ϑ reads

$$\Delta E = 2 \cdot \frac{E_{\mathrm{kin,e}} \cdot m_{\mathrm{e}}}{m_{\mathrm{H_2}}} \cdot (1 - \cos\vartheta). \quad (6)$$

For large energy losses $\Delta E > 100$ eV by ionisation the out-going electron can be treated as quasi-free before the scattering process. Therefore, the correlation between energy loss ΔE and scattering angle ϑ is given by

$$\Delta E = E_{\mathrm{kin,e}} \cdot \left(1 - \cos^2\vartheta\right). \quad (7)$$

For smaller energy losses this approximation is no longer valid and we refer to the description of our detailed energy loss model, which will be discussed in [22]. We would like to note that our energy loss model agrees with exerimental data on the energy loss of 18 keV electrons on molecular hydrogen [23].

Figure 6 presents the energy loss obtained for the simulation of a sample of 10 trapped electrons in the old KATRIN design (see fig. 3). The simulation results show that these electrons lose their transverse energy after each collision event by synchrotron radiation according to eq. (5) on a time scale of less than a second due to the high magnetic field of 5.4 T in the transport magnets.

At a rest gas pressure of 10^{-10} mbar (for technical reasons chosen 10 times higher than that expected for KATRIN), the scattering processes on the rest gas occur at a rate of about 1 per 4 s per stored electron (see fig. 6). As indicated in fig. 4 most processes are elastic or excitation processes without ionisation. Like synchrotron radiation, elastic scattering and excitation processes cool the

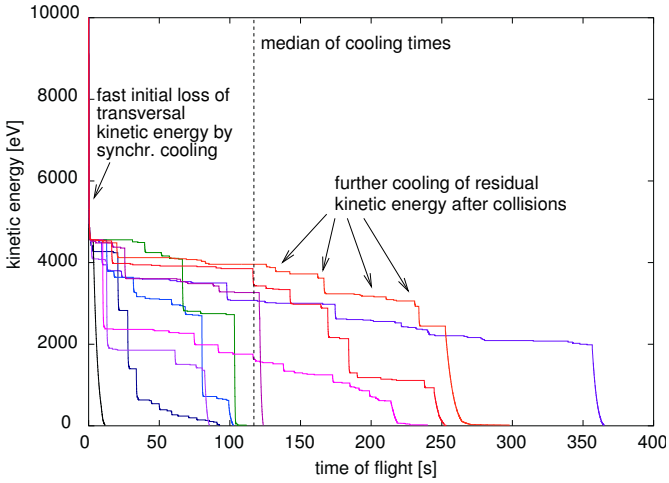


Fig. 6. Simulated energy loss of 10 electrons within the Penning-like trap between the KATRIN pre- and main spectrometers [10]. Energy losses by synchrotron radiation as well as by elastic and inelastic scattering processes on residual H_2 molecules were considered. The electrons started with an energy of $E(0) = 10\,\mathrm{keV}$ halfway between the two spectrometers at a radius of $r = 0.5\,\mathrm{cm}$ and an angle of $\theta = 45°$ with respect to the magnetic field lines. The simulations were performed for a residual gas pressure of $p(H_2) = 10^{-10}\,\mathrm{mbar}$, *i.e.*, 10 times higher than expected for KATRIN. After each collision event the transverse energy is lost by synchrotron radiation within a few seconds, in addition to the energy transfer to the collision partner (sharp steps in the curves). It takes about 100 s (the median of the 10 electrons is 120 s) to cool the electrons down to the ionisation threshold of 15.4 eV.

trapped electron without creating dangerous secondary electron–ion pairs. It should be noted that elastic scattering plays an important role in this cooling process although its corresponding energy loss is small. However, the scattering angle might be large (see eq. 6), redistributing energy from longitudinal to transverse motion, which is radiated away quickly.

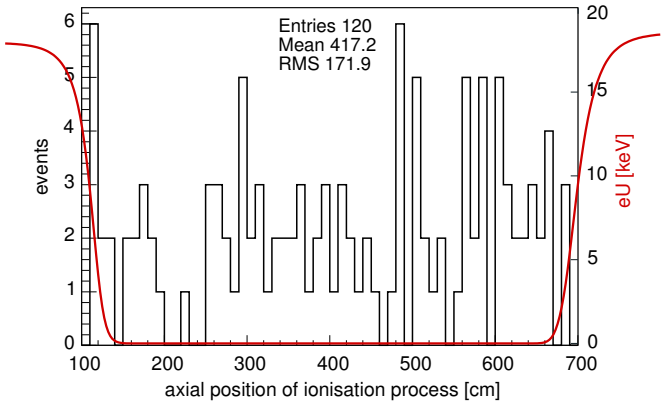


Fig. 7. Position of simulated ionisation events between pre- and main spectrometer on the axis [10]. The full line illustrates the corresponding electric potential (right-hand scale).

Of major concern are the ionisation processes, which occur with a rate of 1 per 10 s per stored electron at the considered rest gas pressure of 10^{-10} mbar. They can start a chain reaction if the secondary electrons obtain a sufficient amount of energy to allow further ionisation, in particular through the subsequent acceleration by the electric field. Figure 7 shows the position on the axis at which the ionisation processes took place for the 10 simulated trapped electrons of fig. 6. Clearly, most ionisation processes take place at ground potential, where no potential energy is picked up. However, a small fraction of the ionisations take place at the end of the trap[7]. In this case, the secondary electrons gain energy from the electric potential and are thus able to further feed the ionisation chain process. To investigate their influence we would have to track these secondary electrons and their tertiary ionisation products further. For the set-up described in the KATRIN design report [3] and the start parameters chosen in the simulations of figs. 6 and 7, on average just one secondary electron is created at a high electric potential per initial trapped electron. This number becomes smaller for larger starting angles and larger for smaller starting angles of the initial electron. Therefore, a significant fraction of initial electrons will create at least one secondary electron and thus will start a chain reaction with a large number of secondary ions N_{ion}.

For the actual KATRIN default design this electron multiplication factor is significantly larger since the transport magnets have been omitted. Just one short solenoid with the beam tube on ground potential connects the pre- and the main spectrometer with their walls on high potential. Consequently the synchrotron cooling is much less efficient and a lot more secondary electrons are created by ionisation processes in the regions of high potential at the end of the trap. In addition, due to the larger track length on high potential, the probability to generate secondary electrons on high potential is larger. Still, the above simulations hold qualitatively and a significant background contribution is expected from this inter-spectrometer trap at KATRIN.

In order to understand this background contribution quantitatively, a significantly scaled-up simulation effort is under way. Trapped electrons and all their secondary and higher scattering products are tracked using the actual KATRIN design. First results show that many positive ions are accelerated into the KATRIN main spectrometer, confirming that this background mechanism is not negligible and requires further investigations and measures. The details of these more advanced simulations will be discussed elsewhere [22] after their finalisation. In this work we will now concentrate on the experimental investigation of this potentially large background.

The most straightforward way to empty the inter-spectrometer electron trap would be to switch off the high voltage temporarily and thus eliminate the trapping con-

[7] Although the track length at high potential is small, the scattering probability is rather large, since the electrons are decelerated by the electric potential and have a larger scattering cross section (see fig. 4).

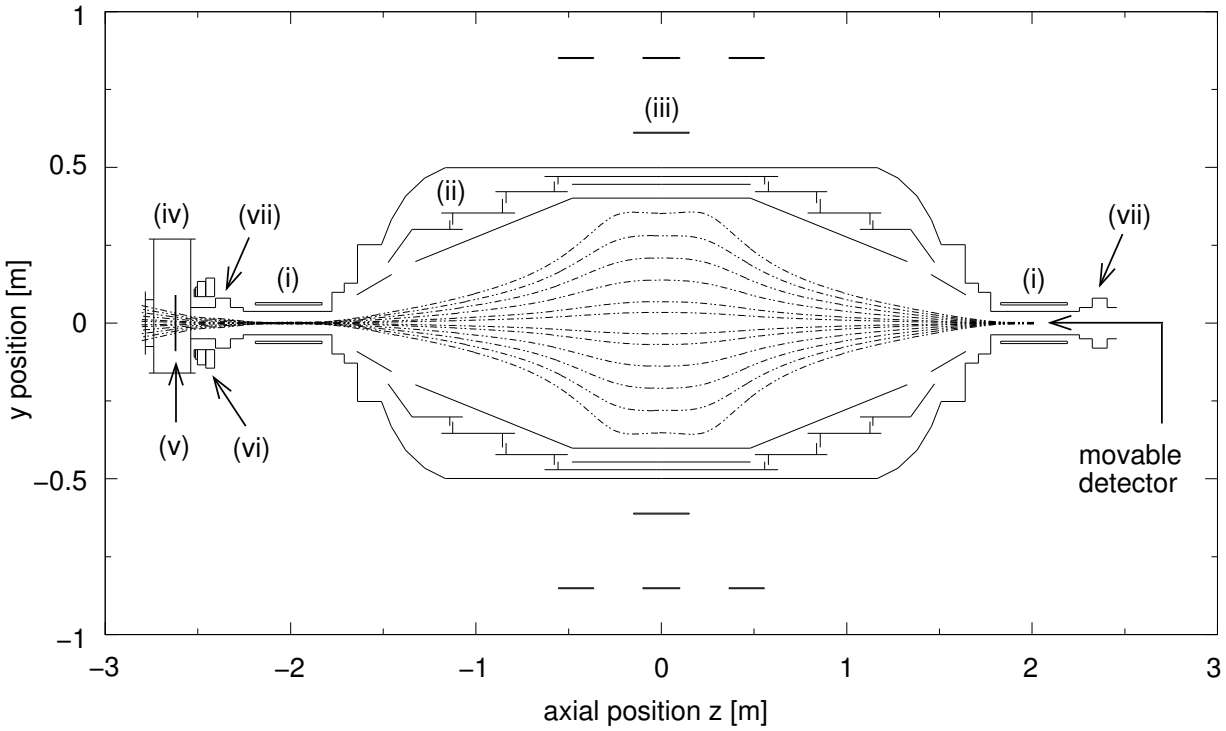


Fig. 8. Set-up used at the Mainz MAC-E filter for testing the trapping conditions between the KATRIN pre- and main spectrometer. (i) superconducting solenoids, (ii) electrode system consisting of vacuum tank at ground potential, solid and inner wire electrode systems on high voltage, (iii) field-shaping air coils, (iv) vacuum chamber housing both the sweeping wire installation and (v) the backplate electrode on high voltage, (vi) water-cooled additional coil for local enhancement of the magnetic field at the position of the sweeping wire (not shown in this drawing), (vii) valves. The detector is situated on a movable sleigh close to the solenoid on the right-hand side. Magnetic field lines (settings corresponding to a resolving power of $B_{max}/B_{min} = E/\Delta E \approx 2 \cdot 10^4$) are indicated as dashed curves.

dition for a short time. During data taking this would have to take place periodically, with short time intervals in between, depending on the fill rate of the trap. However, the abrupt and large change of the high voltage from −18.6 kV to zero and back would be detrimental to the high stability of the high voltage of the main spectrometer and its measurement, which both are required to be better than 50 mV, *i.e.*, 3 ppm, in order to achieve the required sensitivity for the neutrino mass at KATRIN of 0.2 eV/c^2 [3]. Switching the high voltage of the pre-spectrometer down to zero would result in a huge beta electron flux of 10^{10} s^{-1} into the main spectrometer. These electrons would scatter there and induce additional background. The prevention of this is the main purpose of the KATRIN pre-spectrometer. Another way to eject trapped electrons would be to use a transversal electric field, which would remove the electrons by the $\boldsymbol{E}\times\boldsymbol{B}$-drift (see eq. (4)). However, this would require impractically high electric potentials in the case of the KATRIN set-up (≈ 20 kV, [10]). A third way would be the use of a mechanical wire which is rapidly swept through the trap every few seconds during measurement pauses. During a sweep this wire collects electrons that are created and stored in the trap. A sweep of the wire could be easily achieved by applying an electric current pulse through the wire, which would move the wire by virtue of the Lorentz force in the strong axial magnetic field. In the following, we will report on our investigations of this method.

3 Experimental set-up

3.1 Model of the particle trap

The pre- and main spectrometer of KATRIN were not yet available for the tests of this sweeping wire. Therefore, a similar trapping configuration was realised at the spectrometer of the former Mainz neutrino mass experiment [4], which is also a MAC-E filter. The Mainz spectrometer itself was used as stand-in for the KATRIN main spectrometer (fig. 8). The electric potential of the KATRIN pre-spectrometer was emulated by a disc-shaped, mechanically polished stainless steel electrode on high voltage in a vacuum chamber at the entrance of the Mainz MAC-E filter. The magnetic field in between this electrode and the Mainz spectrometer was mainly defined by the superconducting entrance solenoid of the spectrometer ($B_{\max}$ = 6 T). Thus the two negative potentials of the backplate electrode and the MAC-E filter enclose a region of more positive potential where a strong magnetic field is present (fig. 9), thus creating a Penning-like trap for electrons, similar to the case between the pre- and main spectrometer at KATRIN. Typical electron energies at KATRIN

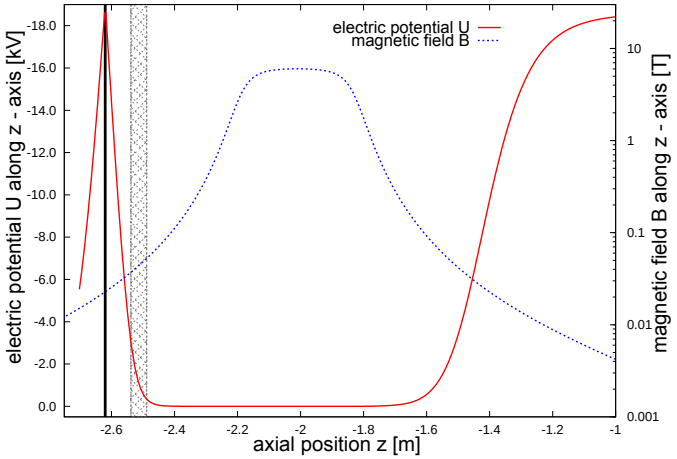


Fig. 9. Electric potential U (solid line) and magnetic field B (dotted line) of the Penning-like trap at the test set-up. the solid vertical bar indicates the position of the disc-shaped electrode; the shaded area marks the region of the sweeping wire.

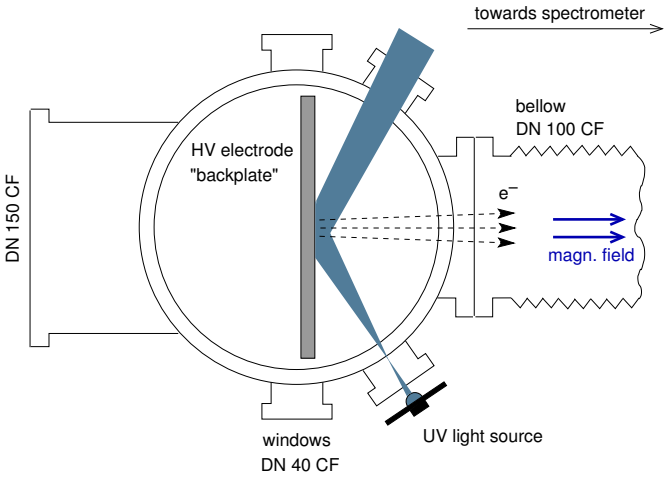


Fig. 10. Top view of the vacuum chamber housing the disc-shaped high-voltage electrode which serves as a stand-in for the KATRIN pre-spectrometer. Electrons can be created in the centre of this electrode by photoemission using UV-light.

are of the order of 18.6 keV with spectrometer voltages of $U_{\mathrm{spec}} \approx -18.6\,\mathrm{kV}$. For this reason the test measurements with this Penning-like trap were made with potentials in the range $-15\,\mathrm{kV}$ to $-18\,\mathrm{kV}$.

A major difference between the electron trap at the KATRIN pre- and main spectrometer and the above test set-up are the magnetic field lines which connect the disc-shaped electrode (cathode plate) with the detector in the latter case. At KATRIN, special care was taken to prevent such a situation, since this can lead to an increased background and a feedback mechanism which can lead to discharges.

3.2 Filling mechanism

Another difference of this set-up compared to KATRIN is the lack of electrons from tritium beta decay[8], which would provide a filling mechanism for the trap. Two different electron sources were used to fill the trap instead. First, the "natural" background of electrons from any electrode surface on negative high potential, caused by field emission, natural radioactivity or cosmic ray interactions, can feed the trap. This comprises the retardation electrodes inside the MAC-E filter as well as the disc-shaped backplate electrode. This mechanism is permanently present and cannot be switched off. A second filling mechanism was provided by photoelectrons directly from the backplate electrode (fig. 10, [24]), which was illuminated by a deep-ultraviolet light emitting diode (UV-LED, Seoul Semiconductor, types T9B25C and T9B26C [25,26], central wavelengths 255 nm and 265 nm.). This led to much higher electron numbers and more efficient and controlled filling of the trap compared to the natural background.

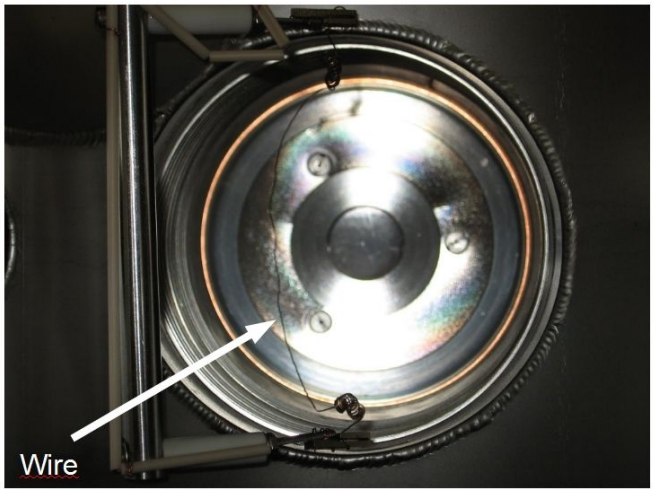
[8] The tritium source of the Mainz neutrino mass experiment has been decommissioned some years ago.

3.3 The sweeping wire

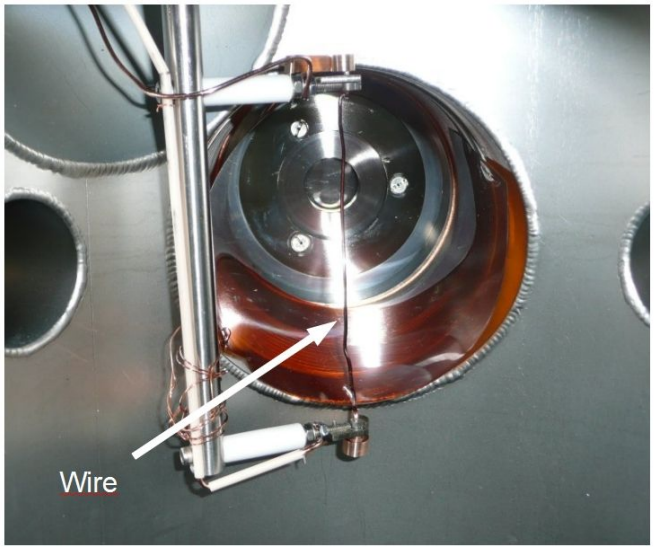
The basic idea to empty the trap consists of a grounded wire that is periodically moved through the trapping region to collect stored charged particles. It is realised with a semi-circle of a copper wire of 0.4 mm or 1.4 mm wire diameter, held by suitable supports to allow rotation through the flux tube covering the detector. The wire motion ranges from wall to wall in the enclosing vacuum chamber (DN100). It is moved back and forth through the flux tube by virtue of the Lorentz force due to a periodic current of $1 - 5\,\mathrm{A}$ through the wire and the local magnetic field of $0.02 - 0.03\,\mathrm{T}$. In order to facilitate the motion of the sweeping wire and to fit the flux tube, which images the plate onto the detector, inside the vacuum tube, the magnetic field was locally enhanced at the position of the sweeping wire with a water-cooled coil (compare fig. 8). The current driving the wire was provided by the output of a function generator amplified by a bipolar operational amplifier (Kepco BOP 20-20M). Using this current the sweeping wire could be swept swiftly through the trap (rectangular modulation of the current), swept slowly through the trap (sine wave modulation of the current), placed at the edge of the flux tube (DC current) or set to the centre of the flux tube (no current). The range of the wire motion covered the whole flux tube (wall to wall). In some of the measurements the timing of the sweeping wire was recorded using the trigger output of the function generator. Figure 11 shows two sweeping wire configurations in position inside the vacuum chamber, looking from the position of the backplate towards the spectrometer.

3.4 Spectrometer settings

The detector used at the exit of the spectrometer to detect electrons from the plate and the trap was a Si-PIN diode (type Hamamatsu S3590-06) of size $9 \times 9\,\mathrm{mm}^2$. The



(a) sweeping wire used in phase I of the measurements. The wire diameter was 0.4 mm.



(b) sweeping wire used in phase II of the measurements. The wire diameter was 1.4 mm.

Fig. 11. Photographs showing two stages of technical realisations of the sweeping wire to empty the Penning-like trap. The pictures were taken from the rear side of the vacuum chamber looking from the backplate towards the spectrometer. The line of sight coincides with the central beam axis. In the background of each picture, the bellow connecting vacuum chamber and spectrometer and the closed gate valve towards the spectrometer are visible. As a common feature, both sweeping wire solutions involve springs to facilitate the motion of the wire and provide an electric current via insulated leads, although they differ in the details of mechanical construction. The final construction used flat spiral springs to conduct the electric current and ultra-high vacuum compatible bearings, which enabled stable long-term operations.

magnetic field at the location of the detector was $B_{\mathrm{det}} = 0.34\,\mathrm{T}$, corresponding to a covered magnetic flux of $\approx 28\,\mathrm{Tmm}^2$. Since the magnetic field at the plate of the photocathode was $0.02 - 0.03\,\mathrm{T}$, an area of $9 - 14\,\mathrm{cm}^2$ of the plate was imaged onto the detector. Typically, measurements were performed at an energy resolution of $\Delta E/E = 1/20000$.

4 Results of the measurements

Measurements of the count rate on the detector were performed under various conditions: without and with trapping conditions present, for the latter case with and without sweeping wire, the sweeping wire in several different operation modes, and for all cases with the spectrometer in transmission as well as closed to low energy electrons from the backplate.

4.1 Behaviour of the count rate without sweeping wire

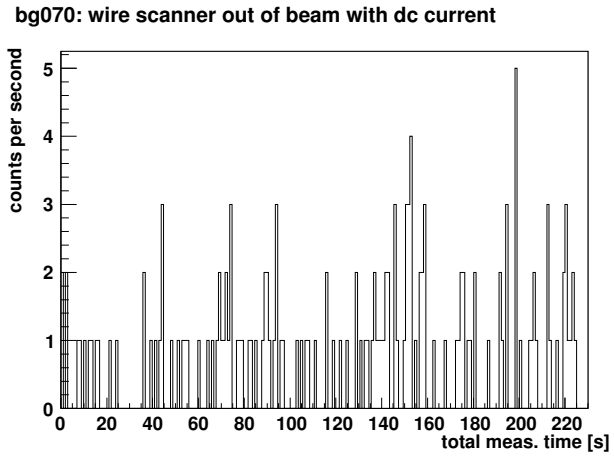
The trap between the backplate and the analysis plane produces several observable effects, depending on the filling mechanism:

4.1.1 Without additional filling of the trap

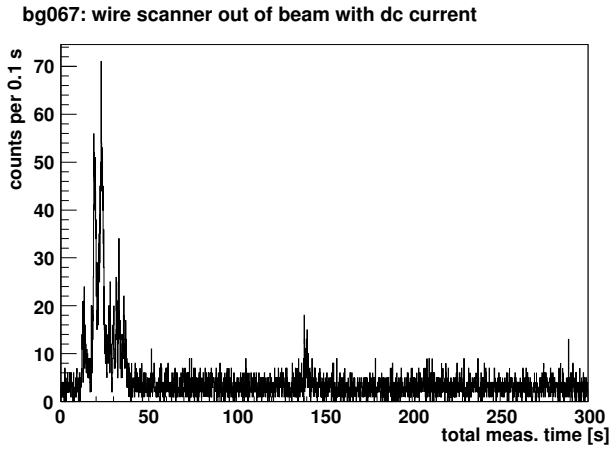
Figure 12 shows the comparison of the count rate for single electrons with and without the trapping condition being present. The trapping condition was switched off by setting the backplate voltage to $U_{\mathrm{plate}} = 0\,\mathrm{V}$. For the case with the trapping condition being present the spectrometer voltage was set to a value so that electrons with very low energy from the backplate could not pass the analysis plane ($U_{\mathrm{plate}} = U_{\mathrm{spec}} + 2$ V with $U_{\mathrm{plate}} \approx -18\,\mathrm{kV}$). In figure 12(a) the natural background of the spectrometer without the trap is shown. The average count rate in the single electron peak of the detector is 0.7 counts/s. This compares with 25 to 35 counts/s for the case where the trap is present, shown in fig. 12(b). In addition to this drastic increase of the count rate frequent and violent bursts were observed when the trap was present. Frequently these led to a strong discharge of the spectrometer and shut down the detector and the spectrometer high voltage due to an excess current (fig. 13).

4.1.2 With photoelectrons

In order to fill the trap in a controlled way photoelectrons were created with the UV-LED off the backplate. The UV-LED was operated in a pulsed mode with a pulse duration of $\tau = 12\ \mu\mathrm{s}$ and a repetition rate of 1000 Hz. When the spectrometer was operated in transmission the time structure of the count rate due to this pulsed operation was clearly visible [24]. Figure 14 shows an example of the development of the count rate with the spectrometer closed ($U_{\mathrm{plate}} \approx U_{\mathrm{spec}} + 9.05\,\mathrm{V}$) and the trapping condition being present. High count rates in the range $1 \cdot 10^3$ counts/s to $3.5 \cdot 10^3$ counts/s were observed. Compared to the count rate due to the natural filling of the trap this is a significant increase of the background. However, no bursts



(a) without high voltage on backplate



(b) with high voltage on backplate

Fig. 12. Evolution of the count rate without and with high voltage on the backplate. In both cases the sweeping wire was positioned outside the magnetic flux tube by applying a constant current; no extra feeding mechanism of the trap was active. (a): Count rate for spectrometer background only ($U_{\mathrm{plate}} = 0$, $U_{\mathrm{spec}} = -18.6$ kV). This leads to a count rate of about 0.7 counts/s. (b): Count rate for $U_{\mathrm{plate}} = U_{\mathrm{spec}} + 2$ V. Strong fluctuations of the count rate on top of a generally elevated level of 25 to 35 counts/s are visible (note the difference in the ordinate).

were visible. A potential explanation is that the bursts were hidden in the elevated (and generally variable) background. The timing of the events is not correlated with the pulses of the UV-LED, indicating that the photoelectrons were at least partially trapped and not directly flying to the detector, which is forbidden by energy conservation.

The fill rate of the trap can be estimated from the count rate when the spectrometer is in transmission. This yields a fill rate of $1.1{\cdot}10^3$ electrons/s to $1.4{\cdot}10^3$ electrons/s. Since the background during quiet periods with trap and photoelectrons present was larger by a factor 2-3 than the fill rate of the trap this means that charge multiplication, a continuous discharge, is taking place in the trap even

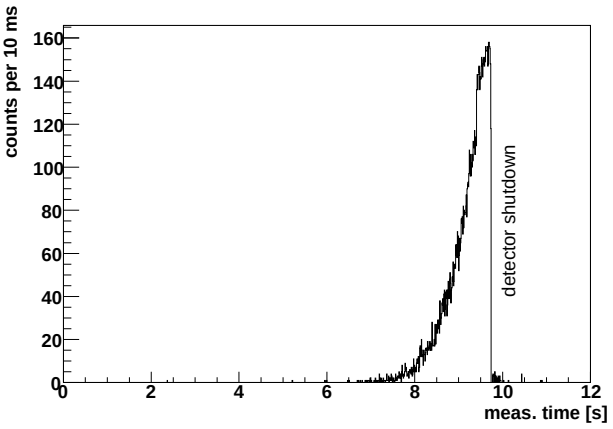


Fig. 13. Example for the build-up of a discharge for the case of natural background only and without intervention of the sweeping wire. After a quick rise of the count rate to about $1.6 \cdot 10^4$ counts/s (limited by the data rate accepted by the data acquisition system) the detector was automatically shut down at $t_{\mathrm{meas}} \approx 9.75$ s.

when no runaway multiplication with resulting detector shutdown is observed.

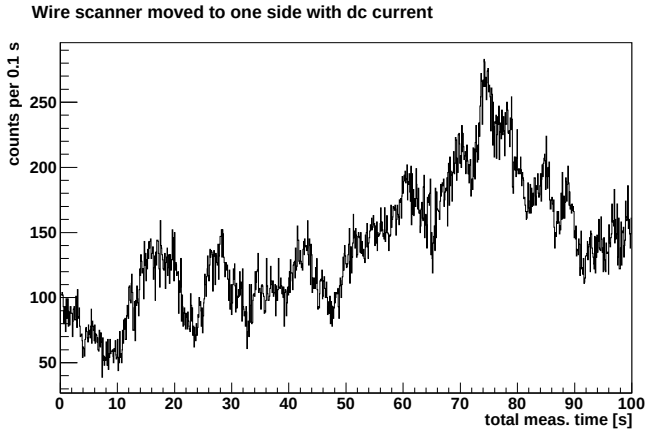


Fig. 14. Count rate with UV photoelectrons as filling mechanism. Voltage setting: $U_{\mathrm{plate}} = -14988.88\,\mathrm{V} \approx U_{\mathrm{spec}} + 9.05\,\mathrm{V}$. The sweeping wire was moved out of the magnetic flux tube with a DC current. High count rates of the order of $1 \cdot 10^3$ counts/s to $3.5 \cdot 10^3$ counts/s were observed. The timing of the events is not correlated with the time of UV emission at the LED.

In summary, the presence of the Penning-like electron trap between the backplate and the analysis plane led to a significant increase of the background count rate as expected from sect. 1, to frequent bursts of the count rate and to frequent strong discharges which shut down the spectrometer and the detector.

4.2 Reduction of background due to the sweeping wire

The effect of the sweeping wire on the count rate from the trap has been investigated for rectangular motion of the wire, sine motion of the wire, and for a wire in fixed position on the axis of the set-up, for the spectrometer electrostatically closed to direct electrons, and for both filling mechanisms.

4.2.1 Natural background

For natural filling the sweeping wire in rectangular mode reduces the count rate during its sweep (fig. 15), evidence that it removes charged particles from the trap, but it is not able to prevent the bursts from building up discharges. This holds even for the fastest sweeping frequencies that were tested ($2-3$ Hz). In addition, the fast current pulse is prone to induce electronic noise in the detector.

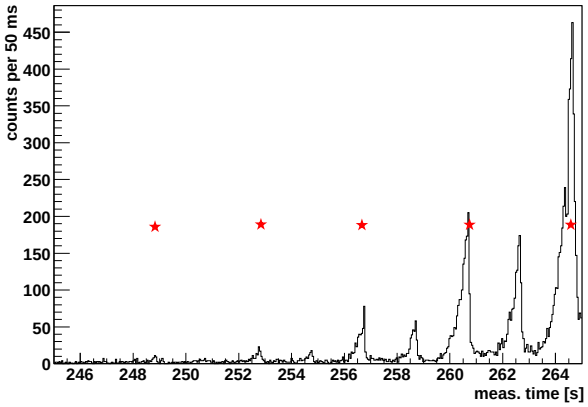


Fig. 15. Build-up of the count rate at the start of a discharge for the case of natural background only and the sweeping wire (1.4 mm wire diameter) active. The trigger signal for the rectangular pulse driving the sweeping wire motion is indicated by red markers. The sweep frequency was $f = 0.3$ Hz. Each trigger signal stands for a sweep of the wire in one direction; the backward sweeps are located in-between two trigger signals at half period and are therefore not shown here. Obviously, the sweeping wire in rectangular mode did not prevent discharges from building up.

The evolution of the background with time for natural filling of the trap and a sinusoidal wire motion with frequency $f = 0.5$ Hz is shown in fig. 16. Both quiet periods and bursts are still visible at this sweeping frequency. In contrast to the background without sweeping wire (fig. 12(b)) the overall count rate is reduced and fewer bursts are visible during the measurement time. When the sweep frequency is reduced bursts start to appear more frequently and get stronger. Figure 17 shows the dependence of the total count rate (averaged over quiet periods and bursts) on the sweep frequency. Clearly, the sweeping wire leads to a strong reduction of the count rate, which implies that it removes charged particles from the trap. For the highest sweep frequency no bursts were visible anymore during the time window of the measurement (600 s).

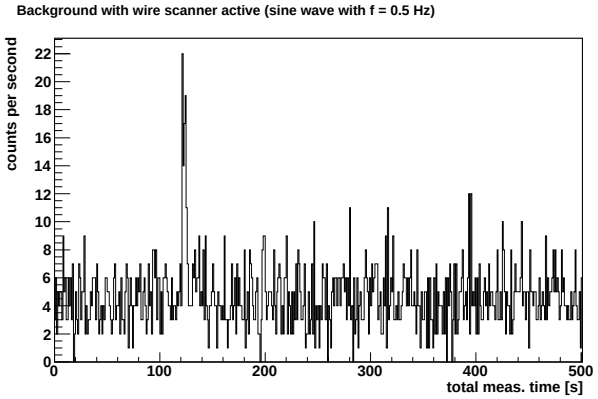


Fig. 16. Count rate for the case of natural background only and the sweeping wire (0.4 mm wire diameter) in sinusoidal mode with frequency $f = 0.5$ Hz.

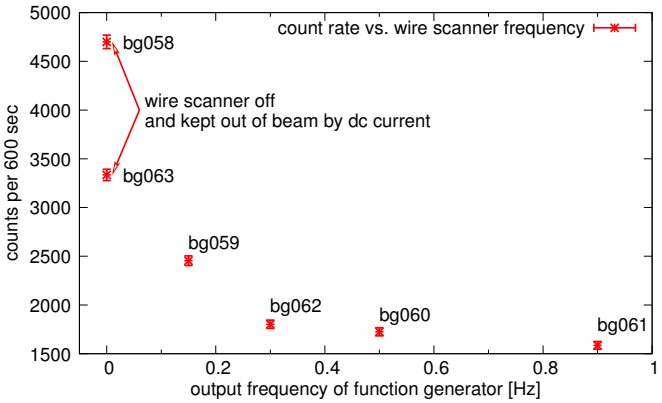


Fig. 17. Count rate at 15 kV for the case of natural background only as a function of the frequency of the sweeping wire (0.4 mm wire diameter) in sinusoidal mode. The difference in counts observed between the measurements with DC current (bg058 and bg063) can be explained by fluctuations of the bursts in the count rate, see time spectra in fig. 16.

Keeping the wire stationary through the centre of the set-up turned out as another effective solution for the suppression of the background and of bursts under the operating conditions used. This method eliminated the strong discharges and most bursts. Only when the spectrometer potential U_{spec} was within several tenths of V of the backplate potential U_{plate} bursts were observed occasionally. The reason why a stationary wire in the centre of the magnetic flux tube works efficiently is the following: Although for this method the wire does not cover the full magnetic flux tube the magnetron motion around the symmetry axis transports the trapped electrons to the wire according to eq. (4), on time scales much less than a millisecond.

4.2.2 With photoelectrons

When filling the trap with photoelectrons from the backplate the background with the sweeping wire removed from the trap region was higher by a factor of ≈ 200 than for the case with natural filling only (compare figs. 12(b) and 14). As in the previous measurements, the sweeping wire in the sine mode results in a significant reduction of the overall rate with the lowest rate being ≈ 100 counts/s at the maximum sweep frequency of 0.5 Hz. Due to the higher count rate here the sweeping wire motion leads to a direct modulation of the count rate (fig. 18). The dependence of the count rate on the frequency of the sweeping motion is also similar, but again at elevated count rates. Having the sweeping wire stationary in the centre reduces the count rate the most to ≈ 10 counts/s. As a further observation, the arrival times of the electrons were not correlated with the UV-LED pulse timing, in contrast to the case of transmission of the spectrometer [24]. This confirms that the remaining low count rate stems from secondary ionisation products of electrons which have been stored in the trap.

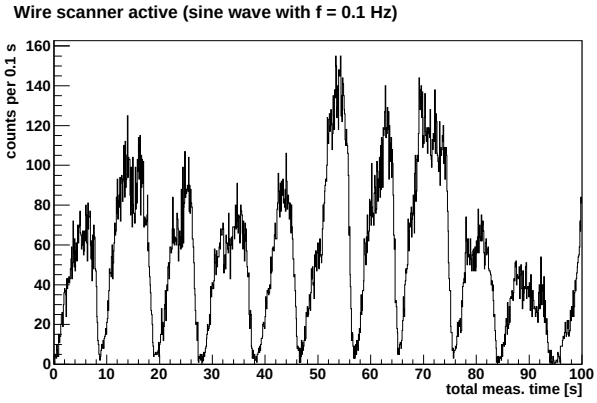


Fig. 18. Count rate with sweeping wire (0.4 mm wire diameter) in sine mode ($f = 0.1$ Hz) with UV photoelectrons as filling mechanism. Voltage setting: $U_{\mathrm{plate}} = -14988.88\,\mathrm{V} \approx U_{\mathrm{spec}} + 9.05\,\mathrm{V}$. The maxima and minima of the count rate correspond to the outer and inner position of the wire, respectively.

4.3 Quenching of discharges

A major problem caused by the trap were discharges which occur after a variable time (see sects. 4.1.1, 4.2.1). Figure 15 shows a typical initial development of such a discharge with the sweeping wire in rectangular mode. After a significant build-up of the discharge the sweeping wire was switched from rectangular mode to slow sine mode at the same frequency (0.3 Hz). This stopped the build-up of the discharge (see fig. 19 and table 1) and an additional increase of the frequency (0.5 Hz) fully extinguished it after some time. This behaviour was reproducible and was repeatedly seen for discharges which, under otherwise similar circumstances, would have led to a gigantic discharge without sweeping wire (compare fig. 13), thereby shutting down the detector and the spectrometer high voltage. The rectangular mode by itself was not sufficient to prevent the discharge from increasing.

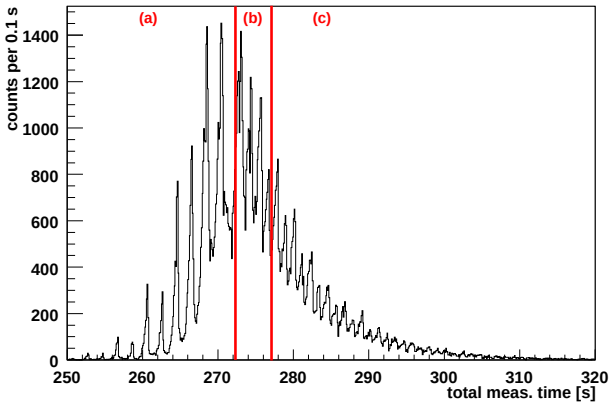


Fig. 19. Influence of sweeping wire motion on an emerging discharge, with UV-photoelectrons (1.4 mm wire diameter). The labels (a), (b) and (c) mark intervals with different sweeping wire settings, see table 1. Clearly, the sweeping wire in fast sine mode will extinguish discharges.

Table 1. Overview of the sweeping wire operation within the different time intervals for the discharge in in fig. 19.

meas. time interval	sweeping wire motion	label
0 – 272 s	rectangular, $f \approx 0.3$ Hz	(a)
272 s – 277 s	sine wave, $f \approx 0.3$ Hz	(b)
277 s – end of run	sine wave, $f \approx 0.5$ Hz	(c)

A very efficient way to quench or prevent discharges from occurring was the sweeping wire in its centre position. This prevented any strong discharges from occurring. Small bursts of the count rate were only seen occasionally close to the edge of transmission. This option was realised at a later stage with a grounded stationary wire crossing the flux tube from wall to wall and going through the central axis. This set up was used to perform test measurements of various photoelectron sources for the calibration of the KATRIN experiment [24,27,28]. The efficacy of the stationary wire again shows the importance of the magnetron drift for the stored electrons.

5 Discussion

It has been shown that a wire, which is swept through a Penning-like trap that creates background electrons by secondary processes outside the trap with a KATRIN-like configuration, reduces that background and can prevent

catastrophic discharges caused by this trap. The background count rate both with and without (fig. 17) injecting photoelectrons depends on the sweeping frequency. Without injecting photoelectrons the minimum achievable count rate was 3 counts/s compared to ≈ 1 counts/s without any trap present, showing that at low fill rate the sweeping wire is highly efficient. A rectangular sweeping motion was not sufficient to prevent discharges. This could only be achieved with a sinusodal wire motion. Additionally, beginning discharges could even be extinguished by switching to a fast sine sweeping motion.

The effectiveness of the sweeping wire and therefore the achievable background count rate depend on the fill rate and the multiplication factor in the trap, *i.e.*, the ionisation time constant. The fill rate was intentionally high in the case discussed here due to the direct field lines from a cathode through the trap caused by the backplate on negative high voltage inside the flux tube. The multiplication factor depends on the residual gas pressure p and the effective path length of the particles in the trap. The former was several 10^{-9} mbar for the measurements discussed here. The effective path length depends on the time scale $\tau_{\mathrm{magnetron}}$ of the magnetron motion of the electrons in the trap, which determines the time until a stored particle will hit the sweeping wire. For the above measurements this time was determined from simulations to be $\tau_{\mathrm{magnetron}} \ll 1$s. High multiplication factors result from large gas pressure p and large magnetron rotation period $\tau_{\mathrm{magnetron}}$, low ones are achieved for small p and small $\tau_{\mathrm{magnetron}}$. For the trap described in figs. 8 and 9 the sweeping wire was sufficiently effective. It can therefore be expected that for similar and less severe trapping situations (filling mechanism, pressure, magnetron time scale) the sweeping wire will be a useful method to reduce the background due to such a trap and to prevent discharges.

Having the sweeping wire fully stationary in the centre of the trap reduces the background rate as well. The count rate was ≈ 10 counts/s with a stationary sweeping wire in the centre when the trap is filled by photoelectrons (sect. 4.2.2). This is a reduction by two orders of magnitude from the count rate observed for photoelectrons without sweeping wire (sect. 4.1.2). Comparison of this count rate with the count rate of ≈ 1 counts/s without any trap present (sect. 4.1.1) shows that the stationary wire significantly reduces the background on the detector caused by the electron trap but does not eliminate it fully. The count rate of ≈ 10 counts/s with stationary wire and with the injection of photoelectrons compares at similar conditions with ≈ 100 counts/s with the sweeping wire at the highest sweep frequencies and with ≈ 30 counts/s without both photoelectrons and without any sweeping wire (sect. 4.1.1), again showing the high effectiveness of the stationary wire. As a consequence of these results a stationary sweeping wire was used for all further experiments at the spectrometer of the former Mainz neutrino mass experiment when the electron trap was present and when the stationary wire in the centre of the beam tube does not harm the measurements. This reliably prevented discharges from occurring for fill rates comparable to the ones discussed here and led to sufficiently low count rates for these experiments (see, *e.g.*, [7,24]).

5.1 Application in the KATRIN experiment

In contrast to the disc-shaped electrode used here, the inter-spectrometer trap at the KATRIN experiment has no cathode connected via magnetic field lines to feed it or to provide an additional amplification mechanism. It will be filled by electrons created in the surrounding electrodes by cosmic rays and natural radioactivity, as well as by electrons from tritium beta decay, which may scatter on residual gas atoms and thus get trapped. The residual gas pressure will be significantly lower than in the above measurement, at $p_{\mathrm{KATRIN}} = 10^{-11}$mbar, and the magnetron motion is calculated to be in the range of $\tau_{\mathrm{magnetron}} = 20 - 200\ \mu$s, comparable with the magnetron motion for the Mainz set-up. This could lead to more favourable multiplication factors at KATRIN than at the above measurements and the efficacy of the sweeping wire could even be better. However, this will strongly depend on the filling mechanism of the trap and must eventually be determined experimentally.

The sweeping wire could be used both in sweeping mode as well as a stationary wire. A stationary wire would form a permanent obstacle and lead to the scattering of electrons[9]. Scattered electrons cannot be used for the measurement of the tritium energy spectrum, meaning that the detector pixels on which the sweeping wire is imaged have to be discarded, leading to a loss of statistics. A sweeping wire operated in sine mode would have the same problem, but has the advantage that it could be fully removed from the beam or centred in the flux tube like a stationary wire. However, if the electron multiplication in the trap should be sufficiently small then the sweeping wire could be operated with pauses between two periods of the sine or even in rectangular mode. The measurement of the tritium beta spectrum would take place while the sweeping wire is outside the flux tube imaged onto the detector. Similarly a stationary wire could be inserted into the centre of the beam tube periodically separated by time intervals without wire. Again, this has to be investigated experimentally in the final configuration at the KATRIN set-up.

5.2 Outlook: potential applications at other experiments

Besides the KATRIN experiment there are other experiments which suffer from unintended particle traps causing an increase of the background level or discharges (*e.g.*,

[9] It would be a mechanical obstacle: since it is located in between the spectrometers, where the electric potential is close to zero, and the wire itself is on ground potential it should not influence the trajectories of electrons from tritium decay that do not hit it directly. However, a fraction of $\approx 17\%$ of the pixels of the KATRIN Si-PIN detector would be covered by the shadow of the wire.

in the area of fundamental interaction investigations the WITCH experiment [29,30], the aSPECT experiment [31] and the NAB experiment [32]). The sweeping wire technique discussed here may also be of use at these experiments.

This work was supported by the German Federal Ministry of Education and Research under grant number 05 CK5 MA/0. One of the authors (M. Z.) was also supported by the MSMT, Czech Republic under the contract LA318. We wish to thank the members of AG Quantum/Institut für Physik, Johannes Gutenberg-Universität Mainz, for their kind hospitality and for giving us the opportunity to carry out these measurements in their laboratory.

References

1. E. W. Otten and C. Weinheimer, *Neutrino mass limit from tritium β decay*, Rep. Prog. Phys. **71** (2008) 086201, doi:10.1088/0034-4885/71/8/086201
2. J. Lesgourgues and S. Pastor, *Massive neutrinos and cosmology*, Phys. Rep. **429** (2006) 307 , doi:10.1103/PhysRevD.79.045026
3. The KATRIN collaboration (J. Angrik *et al.*), *KATRIN Design Report 2004*, FZKA Scientific Report 7090, 2005, available online at `http://bibliothek.fzk.de/zb/berichte/FZKA7090.pdf`
4. A. Picard *et al.*, *A solenoid retarding spectrometer with high resolution and transmission for keV electrons*, Nucl. Instr. Meth. **B 63** (1992) 345, doi:10.1016/0168-583x(92)95119-c
5. V. M. Lobashev and P. E. Spivak, *A method for measuring the electron antineutrino rest mass*, Nucl. Instr. Meth. **A 240** (1985) 305, doi:10.1016/0168-9002(85)90640-0
6. K. Blaum, *High-accuracy mass spectrometry with stored ions*, Phys. Rep. **425** (2006) 1, doi:10.1016/j.physrep.2005.10.011
7. K. Valerius, *Spectrometer-related background processes and their suppression in the KATRIN experiment*, dissertation, Westfälische Wilhelms-Universität Münster, 2009
8. F. Habermehl, *Electromagnetic Measurements with the KATRIN Pre-Spectrometer*, dissertation, Universität Karlsruhe, 2009
9. T. Tabata and T. Shirai, *Analytic cross sections for collisions of H^+, H_2^+, H_3^+, H, H_2 and H^- with hydrogen molecules*, Atomic Data and Nuclear Data Tables **76** (2000) 1-25, doi:10.1006/adnd.2000.0835
10. K. Essig, *Untersuchungen zur Penningfalle zwischen den Spektrometern des KATRIN-Experiments*, diploma thesis, Rheinische Friedrich-Wilhelms-Universität Bonn, 2004
11. Th. Thümmler, *Entwicklung von Methoden zur Untergrundreduzierung am Mainzer Tritium-Beta-Spektrometer*, diploma thesis, Johannes Gutenberg-Universität Mainz, 2002
12. B. Flatt, *Designstudien für das KATRIN Experiment*, diploma thesis, Johannes Gutenberg-Universität Mainz, 2001
13. SIMION Version 7.0, Scientific Instruments Services Inc, 1027 Old York Road, Ringoes, New York 08551, USA, `http://simion.com`
14. J. D. Jackson, *Classical Electrodynamics*, John Wiley & Sons Inc., 1998
15. S. Trajmar, D. F. Register and A. Chutjian, *Electron scattering by molecules II. Experimental methods and data*, Phys. Rep. **97** (1983) 219, doi:10.1016/0370-1573(83)90071-6
16. J. W. Liu, *Total cross sections for high-energy electron scattering by H2(1Σg+), N2(1Σg+), and O2(3Σg−)*, Phys. Rev. **A 35** (1987) 591, doi:10.1103/PhysRevA.35.591
17. G. P. Arrighini, F. Biondi and C. Guidotti, *A study of the inelastic scattering of fast electrons from molecular hydrogen*, Mol. Phys. **41** (1980) 1501
18. Zhifan Chen, A. Z. Msezane, *Calculation of the excitation cross sections for the $^1\Sigma_u^+$ and $C^1\Pi_u^+$ states in $e - H_2$ scattering at 60 eV*, Phys. Rev. **A 51** (1995) 3745, doi:10.1103/PhysRevA.51.3745
19. W. Hwang, Y.-K. Kim and M. E. Rudd, *New model for electron-impact ionization cross sections of molecules*, J. Chem. Phys. **104** (1996) 2956
20. J. W. Liu, *Total Inelastic Cross Section for Collisions of H2 with Fast Charged Particles*, Phys. Rev. **A 7** (1973) 103, doi:10.1103/PhysRevA.7.103
21. I. Wolff, *Entfaltung der Energieverlustfunktion beim KATRIN Experiment*, diploma thesis, Westfälische Wilhelms-Universität Münster, 2008
22. F. Glück, *to be published*
23. V. N. Aseev *et al.*, *Energy loss of 18 keV electrons in gaseous T_2 and quench condensed D_2 films*, Eur. Phys. J. **D 10** (2000) 39, doi:10.1007/s100530050525
24. K. Valerius, M. Beck, H. Arlinghaus, J. Bonn, V. M. Hannen, H. Hein, B. Ostrick, S. Streubel, Ch. Weinheimer and M. Zbořil, *A UV LED-based fast-pulsed photoelectron source for time-of-flight studies*, New J. Phys. **11** (2009) 063018, doi:10.1088/1367-2630/11/6/063018
25. Seoul Semiconductor Co., Ltd., *Specification document for UV LED model series T9B25* (Rev. 1.0)*, 2006, `http://www.socled.com`
26. Seoul Semiconductor Co., Ltd., *Specification document for UV LED model series T9B26* (Rev. 2.0)*, 2006, `http://www.socled.com`
27. K. Valerius, M. Beck, H. Baumeister, J. Bonn, H. Hein, K. Hugenberg, B. Ostrick, M. Zbořil, and C. Weinheimer, *Prototype of an angular-defined photoelectron calibration source for the KATRIN experiment, in preparation*
28. K. Hugenberg, M. Beck, S. Bauer, H. Baumeister, J. Bonn, H. Hein, B. Ostrick, S. Rosendahl, S. Streubel, K. Valerius, M. Zbořil, and C. Weinheimer, *An angular selective photoelectron calibration source for the KATRIN experiment with high angular resolution, in preparation*
29. M. Beck *et al.*, *WITCH: a recoil spectrometer for weak interaction and nuclear physics studies*, Nucl. Instr. Meth. **A 503** (2003) 567, doi:10.1016/s0168-9002(03)00994-x
30. V. Yu. Kozlov *et al.*, *The WITCH experiment: Acquiring the first recoil ion spectrum*, Nucl. Instr. Meth. **B 266** (2008) 4515, doi:10.1016/j.nimb.2008.05.150

31. F. Glück *et al.*, *The neutron decay retardation spectrometer aSPECT: electromagnetic design and systematic effects*, Eur. Phys. J. **A 23** (2005) 135, doi:10.1140/epja/i2004-10057-1
32. D. Počanić *et al.*, *Nab: Measurement Principles, Apparatus and Uncertainties*, Nucl. Instr. Meth. **A 611** (2009) 211, doi:10.1016/j.nima.2009.07.065